Spinal Codes Over Fading Channel: Error Probability Analysis and Encoding Structure Improvement

Aimin Li, *Graduate Student Member, IEEE*, Shaohua Wu, *Member, IEEE*, Jian Jiao, *Member, IEEE*, Ning Zhang, *Senior Member, IEEE*, and Qinyu Zhang, *Senior Member, IEEE*

***Abstract*— In order to facilitate the reliability of data transmission of Spinal codes over the fading channel, performance analysis of Spinal codes is conducted, and an improved encoding structure is proposed. First, we derive an approximate frame error rate (FER) upper bound for Spinal codes over the Rayleigh fading channel in the finite block length (FBL) regime. Then, inspired by the FER analysis process, we propose an improved encoding structure, named self-concatenation structure, to reduce the FER of Spinal codes. In addition, a parallel structure is proposed for Spinal codes to improve the decoding throughput. For the self-concatenation structure, simulation results show that it exhibits a significant gain in anti-noise performance compared with the original Spinal codes over the Rayleigh fading channel. For the parallel structure, we find that by combining the parallel structure with the self-concatenation structure, not only is the encoding and decoding throughput of Spinal codes significantly improved but also the FER of Spinal codes is reduced.**

***Index Terms*— Spinal codes, FER analysis, Rayleigh fading channel, encoding structure improvement.**

I. Introduction

SPINAL codes are a new kind of capacity-approaching rateless code which has attracted extensive research interest because of its simple coding structure and outstanding rate performance [1]–[3]. The coding structure of Spinal codes is very simple. It generates uniformly distributed code words with pseudo-random characteristics by combining a hash function with a random number generator (RNG). Its general idea originates from the concept of random codes proposed by Shannon. By pseudo-random coding, both the anti-noise ability and the robustness of information transmission are enhanced.

Due to the rateless characteristic, Spinal codes hold great potential research value in the field of wireless communications. Different from conventional fixed-rate codes which need to select a specific code length according to the channel characteristics, rateless code forms a variable-length encoding characteristic. It can adaptively generate as many coded symbols as needed by a fixed input message sequence. At the receiver end, the decoder can recover the message sequence once sufficient channel output symbols are received. Therefore, rateless code can be regarded as an adaptive-coded-modulation (ACM) technique, which gives rise to its remarkable potential value to be applied in wireless communications. The first practical rateless code is LT code [4], [5], which is designed for the binary erasure channel (BEC). Then, on the basis of LT code, the state-of-the-art Raptor code is proposed [6], [7]. Raptor code concatenates LT code as outer code with LDPC code, which further reduces the decoding complexity and improves the error correction performance of LT code. Since then, rateless code has drawn extensive research interest due to its excellent adaptive channel characteristics. Many new kinds of rateless code are designed, such as Kite codes [8], [9], reconfigurable rateless code [10], and analog fountain codes (AFC) [11]. Even some fixed-rate codes have been modified to obtain a form of rateless transmission scheme [12]. Spinal codes are a new class of rateless code which do not need to frequently estimate the channel state to adjust the code rate and modulation mode. Instead, it keeps generating and transmitting pseudo-random coded symbols until the decoding process is successful and an acknowledgment (ACK) is fed back to the transmitter to interrupt the symbol transmission.

Theoretical performance analysis of Spinal codes in the FBL regime is a fundamental prerequisite for the analytical design of Spinal-codes-based high-efficiency techniques. To improve Spinal codes under wireless communication scenarios, theoretical performance analysis is a primary need. In [3], Spinal codes' theoretical performance over the additive white Gaussian noise channel (AWGN) and the binary symmetric channel (BSC) is discussed, wherein the capacity achievability of Spinal codes is proved, and a general idea of asymptotic

Manuscript received December 2, 2020; revised April 5, 2021 and May 31, 2021; accepted June 12, 2021. Date of publication June 30, 2021; date of current version December 10, 2021. This work was supported in part by the National Natural Science Foundation of China under Grant 61871147, Grant 62071141, Grant 61831008, and Grant 61371102; in part by the Shenzhen Municipal Science and Technology Plan under Grant GXWD20201230155427003-20200730122528002; and in part by the Guangdong Science and Technology Planning Project under Grant 2018B030322004. The associate editor coordinating the review of this article and approving it for publication was G. Fodor. *(Corresponding author: Shaohua Wu.)*

Aimin Li, Shaohua Wu, Jian Jiao, and Qinyu Zhang are with the Department of Electronic Engineering, Harbin Institute of Technology, Shenzhen 518055, China (e-mail: hitliaimin@163.com; hitwush@hit.edu.cn; jiaojian@hit.edu.cn; zqy@hit.edu.cn).

Ning Zhang is with the Department of Electrical and Computer Engineering, University of Windsor, Windsor, ON N9B 3P4, Canada (e-mail: ning.zhang@uwindsor.ca).

Color versions of one or more figures in this article are available at https://doi.org/10.1109/TWC.2021.3091719.

Digital Object Identifier 10.1109/TWC.2021.3091719

error probability analysis of Spinal codes is given. In [13], the authors derive the upper bound of FER for each priority of UEP Spinal codes in the FBL regime over the AWGN channel and the BSC, which is the first work on non-asymptotic performance analysis of Spinal codes. In [14], a tighter FER upper bound for Spinal codes over the BSC is derived, which fits better with the FER simulation results of Spinal codes than that in [13]. The theoretical research on Spinal codes under the AWGN channel and the BSC is developing rapidly and becoming more and more mature. However, related theoretical research of Spinal codes over fading channels remains deficient. In this paper, we will analyze the theoretical FER performance of Spinal codes under the FBL regime over fading channels. To our best knowledge, this is the first research on error probability analysis with regard to Spinal codes over fading channels.

Although Spinal codes hold advantages of the capacity-achieving property and the ACM characteristics, there are still some problems to be solved. Specifically, Spinal codes' error correction ability over wireless channels is still weak; Spinal codes' decoding algorithm still needs to be improved due to its high decoding complexity; Spinal codes' coding and decoding throughput are insufficient because of its serial coding structure. To solve these problems, amounts of work has been done for Spinal codes on its way from theory to practice, which can be found in [15]–[19]. However, most of the existing research tends to improve the performance of Spinal codes in the long or medium length of the block length. In 5G application scenarios, the transmission under the short block length regime has become a requirement. For Spinal codes in the short length of the block length, the coding structure needs to be further optimized.

In this paper, a new Spinal codes' structure is proposed, which is called self-concatenation Spinal codes. We begin with analyzing the FER upper bound for Spinal codes over the Rayleigh fading channel. Then, inspired by the FER analysis process, the proposed self-concatenation Spinal codes is introduced, combined with its related FER analysis. Finally, considering that maximum likelihood (ML) decoding algorithm under self-concatenation Spinal codes is with high complexity when the length of information sequence increases, the parallel self-concatenation Spinal codes is proposed, which not only improves the encoding and decoding throughput of Spinal codes but also reduces the FER of Spinal codes.

The main contributions of this work can be summarized as follows:

- We derive a non-asymptotic (FBL) approximate FER upper bound for Spinal codes over the Rayleigh fading channel, which is the first work on performance analysis of Spinal codes over fading channels.
- Based on the theoretical FER analysis, the self-concatenation Spinal codes is proposed, which immensely improves the FER performance of Spinal codes.
- We propose the parallel self-concatenation structure of Spinal codes, which improves both the FER performance and the decoding efficiency of Spinal codes.

The rest of this paper is organized as follows. Section II introduces preliminaries of Spinal codes. In Section III, the FER upper bound of Spinal codes over the Rayleigh fading channel is derived. The details of the coding and decoding process of self-concatenation Spinal codes are presented in Section IV, in which the FER analysis of self-concatenation Spinal codes is also given. In Section V, the proposed parallel self-concatenation Spinal codes is presented. Simulation results are shown in Section VI, followed by conclusions in Section VII.

II. Related Works

A. Encoding Structure of Spinal Codes

The encoding process of Spinal codes can be divided into 4 steps.

Step 1: An n-bit message M is divided into n/k k-bit segments, denoted by m_i, where $i \in \{1, 2, \ldots, n/k\}$.

Step 2: The encoder calls hash function iteratively to map the message segment m_i to a v-bit hash state s_i as

$$s_i = h(s_{i-1}, m_i), \quad s_0 = 0^v, \tag{1}$$

where s_0 serves as the initial hash state known by both the encoder and the decoder, $v = 32$ in the simulation of this paper.

Step 3: The v-bit hash state s_i is input to the RNG as a seed to generate pseudo-random c-bit symbols denoted by $x_{i,j}$:

$$\mathrm{RNG}: s_i \rightarrow x_{i,j}, \tag{2}$$

where $x_{i,j} \in \{0,1\}^c$, $s_i \in \{0,1\}^v$.

Step 4: The encoder maps the c-bit symbols to a channel input set to fit the channel characteristics:

$$\mathrm{f}: x_{i,j} \rightarrow \Omega, \tag{3}$$

where f is a constellation mapping function, Ω is the channel input set. In this paper, our theoretical research and performance simulation are all carried out under the condition of uniform constellation mapping with $\mathrm{f}(x) = x$. Fig. 1 shows an example with $n/k = 8$.

B. Decoding Algorithm of Spinal Codes

The optimal decoding algorithm for Spinal codes is ML decoding. In ML decoding, the decoder utilizes the shared knowledge of the same hash function, the same initial hash state value s_0, and the same RNG to replay the coding process. In short, the decoder aims to find the best matching sequence $\hat{M} \in \{0,1\}^n$ whose encoded vector $\mathbf{x}(\hat{M})$ is closest to the received vector $\mathbf{y}$ in Euclidean distance. The mathematical form of ML rule can be expressed as

$$\begin{aligned} \hat{M} &= \underset{M' \in \{0,1\}^n}{\arg\min} \|\mathbf{y} - \mathbf{x}(M')\| \\ &= \underset{M' \in \{0,1\}^n}{\arg\min} \sum_{i=1}^{n/k} \sum_{j=1}^{l_i} \|y_{i,j} - x_{i,j}(M')\|, \end{aligned} \tag{4}$$

where $\hat{M}$ denotes the decoding result, M' represents the candidate sequence and l_i is the number of symbols generated from the i^{th} hash state value s_i of the n-bit message M.

However, traversing all candidate sequences results in an exponential increase in complexity. The serial coding structure

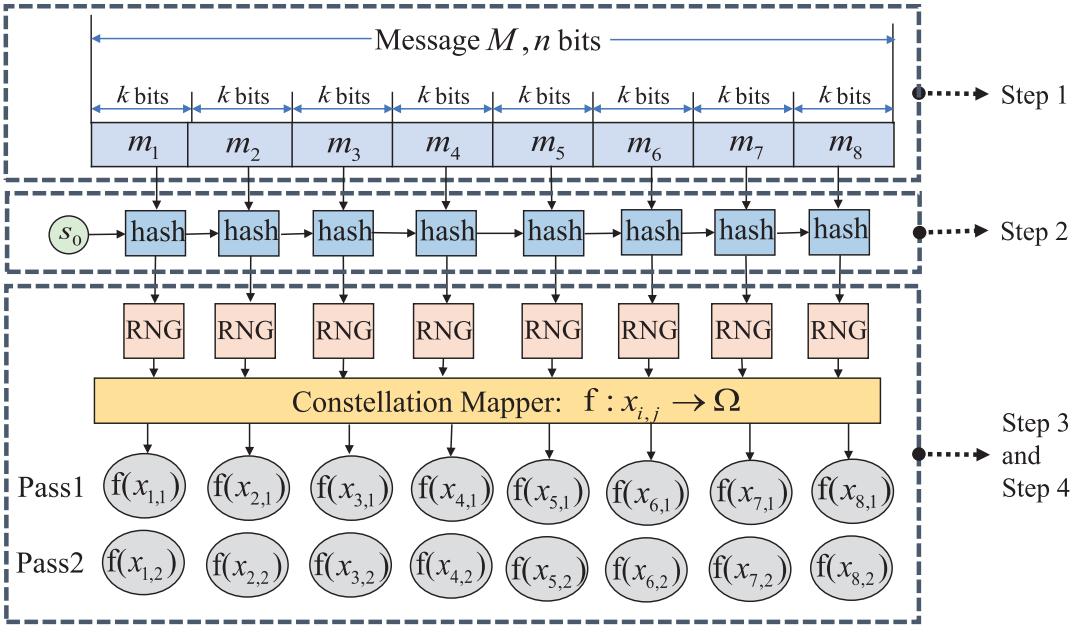

Fig. 1. The encoding process of Spinal codes.

of Spinal codes determines that Spinal codes are a type of tree code. As a result, the tree pruning decoding algorithm named bubble decoding can be applied to decrease the decoding complexity [2].

III. FER Upper Bound Analysis Over the Rayleigh Fading Channel

Theoretical performance analysis of Spinal codes under the FBL regime is a fundamental prerequisite for the analytical design of Spinal-codes-based high-efficiency techniques. In this section, we derive a non-asymptotic approximate FER upper bound for Spinal codes over the Rayleigh fading channel. We begin with briefly introducing the Rayleigh fading channel model and then derive the FER upper bound for Spinal codes over it.

A. Rayleigh Fading Channel

Rayleigh fading channel model can effectively describe the wireless propagation environment with obstacles that can scatter a large number of radio signals. In a terrestrial mobile communication system, the channel can be generally modeled as a Rayleigh fading channel. Generally, the receiver must firstly detect and demodulate the data when receiving the symbols. After these processing steps, the fading in a code block can be generally reduced to flat fading. The mathematical channel model can be expressed as

$$y_{i,j} = r_{i,j} e^{j\phi} x_{i,j}(M) + n_{i,j}, \tag{5}$$

where $y_{i,j}$ denotes the received symbol, $x_{i,j}(M)$ is the coded symbol of message sequence M, ϕ is uniformly distributed over $(0, 2\pi)$ and $r_{i,j}$ obeys Rayleigh distribution with

$$p(r_{i,j}) = \begin{cases} \frac{r_{i,j}}{{\sigma_1}^2} e^{-\frac{{r_{i,j}}^2}{{\sigma_1}^2}} & r_{i,j} \geq 0 \\ 0 & r_{i,j} < 0. \end{cases} \tag{6}$$

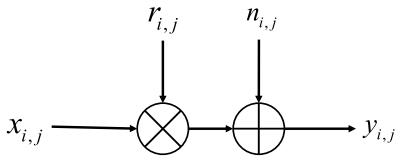

Fig. 2. Flat slow Rayleigh fading channel.

Consider a slow fading channel. The receiver will compensate the received signal after coherent demodulation, matched filtering, and sampling. And then, $\phi \approx 0$ and we can simplify the model as

$$y_{i,j} = r_{i,j} x_{i,j}(M) + n_{i,j}. \tag{7}$$

Fig. 2 shows a flat slow Rayleigh fading channel model. In the next subsection, we will approximate the non-asymptotic FER upper bound for Spinal codes under this model.

B. FER Upper Bound Approximation

Theorem 1 FER Upper Bound Approximation for Spinal Codes Over the Rayleigh Fading Channel: Consider Spinal codes with message length n, segmentation parameter k and modulation parameter c transmitted over an Rayleigh fading channel with noise variance σ^2 and Rayleigh parameter σ_1. The FER under ML decoding can be approximately upper bounded by

$$P_e \lessapprox 1 - \prod_{a=1}^{n/k} (1 - \epsilon_a), \tag{8}$$

with

$$\epsilon_a = \min\left\{1, \left(2^k - 1\right) 2^{n-ak} \cdot \min\left(1, R_a\right)\right\}, \tag{9}$$

where R_a can be calculated by (10), shown at the bottom of the page.

In (10), $\Gamma(\cdot)$ denotes the Gamma function. l_i is the number of symbols generated from the i^{th} hash state value s_i.

The proof of Theorem 1 can be succinctly divided into 3 parts. Recall that the ML decoder aims to find the most matching candidate sequences in M' as the decoding output, we begin with investigating the set of candidate sequences and classify it into two subsets: M'_{c} and M'_{w}. This part is labeled by **Candidate Sequences Classification** in the proof. Second, we analyze the cost of correct candidate sequence $D\left(m'_{\mathrm{c}}\right)$ and $D_a\left(m'_{\mathrm{c}}\right)$, which is labeled by **Cost Analysis of Correct Sequences**. At last, we analyze the cost of wrong candidate sequence $D\left(m'_{\mathrm{w}}\right)$, which is labeled by **Cost Analysis of Wrong Sequences**.

Proof: 1) Candidate Sequences Classification: Suppose that message $M = \left(m_1, m_2 \ldots, m_{n/k}\right)$. Let $x_{i,j}(M)$ denote the j^{th} coded symbol generated from the i^{th} hash state value s_i of the n-bit message M, $y_{i,j}$ denote the corresponding symbol received by the receiver, and $n_{i,j}$ represent the corresponding white Gaussian noise. Over a flat slow Rayleigh fading channel, it is easy to obtain that

$$y_{i,j} = r_{i,j} x_{i,j}\left(M\right) + n_{i,j}. \tag{11}$$

For Spinal codes over the Rayleigh fading channel, ML decoding algorithm is straightforward, with

$$\begin{aligned}\hat{M} &= \underset{M' \in \{0,1\}^n}{\arg\min} \left\|\mathbf{y} - \mathbf{x}(M')\right\| \\ &= \underset{M' \in \{0,1\}^n}{\arg\min} \sum_{i=1}^{n/k} \sum_{j=1}^{l_i} \left\|y_{i,j} - x_{i,j}(M')\right\|, \end{aligned} \tag{12}$$

where M' denotes the candidate sequence and l_i is the number of symbols generated from the i^{th} hash state value s_i of the n-bit message M.

We classify the candidate sequence set into two subsets: M'_{c} and M'_{w}. The subset M'_{c} is defined by

$$M_{\mathrm{c}}{}' = \left\{ m_{\mathrm{c}}{}' \middle| \, m_{\mathrm{c}}{}' = M \right\}, \tag{13}$$

and the subset M'_{w} is defined by

$$M_{\mathrm{w}}{}' = \left\{ m_{\mathrm{w}}{}' \middle| \, m_{\mathrm{w}}{}' \neq M \right\}. \tag{14}$$

2) Cost Analysis of Correct Sequences: Second, we analyze the cost of the candidate sequence in M'_{c}. The candidate sequence in M'_{c} is unique with $m'_{\mathrm{c}} \in M'_{\mathrm{c}}$. The cost of it is denoted by $D(m'_{\mathrm{c}})$ and can be calculated as follows.

$$\begin{aligned} D(m'_{\mathrm{c}}) &= \sum_{i=1}^{n/k} \sum_{j=1}^{l_i} \left(y_{i,j} - x_{i,j}\left(m'_{\mathrm{c}}\right)\right)^2 \\ &= \sum_{i=1}^{n/k} \sum_{j=1}^{l_i} \left(r_{i,j} x_{i,j}\left(M\right) + n_{i,j} - x_{i,j}\left(M\right)\right)^2 \end{aligned} \tag{15}$$

We assume that $r_{i,j}$ is independently and identically distributed (i.i.d). Then, it holds that

$$\begin{aligned} &\mathbb{E}\left(\left(r_{i,j} x_{i,j}\left(M\right) + n_{i,j} - x_{i,j}\left(M\right)\right)^2\right) \\ &\quad = \frac{\left(2{\sigma_1}^2 - \sqrt{2\pi}\sigma_1 + 1\right)\left(2^c + 1\right)\left(2^c - 1\right)}{12} + \sigma^2. \end{aligned} \tag{16}$$

To pave the way for the rest of the proof, we introduce a definition $D_a(m'_{\mathrm{c}})$ here with

$$D_a(m'_{\mathrm{c}}) = \sum_{i=a}^{n/k} \sum_{j=1}^{l_i} \left(r_{i,j} x_{i,j}\left(M\right) + n_{i,j} - x_{i,j}\left(M\right)\right)^2. \tag{17}$$

Denote the right hand side of (16) as $g\left(\sigma, \sigma_1\right)$. The mathematical expectation of (15) and (17) can be calculated using

$$\begin{aligned} \mathbb{E}\left(D(m'_{\mathrm{c}})\right) &= g\left(\sigma, \sigma_1\right) \sum_{i=1}^{n/k} l_i \\ \mathbb{E}\left(D_a(m'_{\mathrm{c}})\right) &= g\left(\sigma, \sigma_1\right) \sum_{i=a}^{n/k} l_i. \end{aligned} \tag{18}$$

By applying the chernoff bound, we can obtain that for $\forall \varepsilon \geq 0$, it holds that

$$\begin{aligned} &\mathbb{P}\left(D\left(m_{\mathrm{c}}{}'\right) \leqslant (1+\varepsilon) \sum_{i=1}^{n/k} l_i g\left(\sigma, \sigma_1\right)\right) \\ &\qquad \geqslant 1 - \left(\frac{e^{\varepsilon}}{(1+\varepsilon)^{1+\varepsilon}}\right)^{\sum_{i=1}^{n/k} l_i g(\sigma, \sigma_1)}. \end{aligned} \tag{19}$$

This means that we possess probability of at least $1 - \left(\frac{e^{\varepsilon}}{(1+\varepsilon)^{1+\varepsilon}}\right)^{\sum_{i=1}^{n/k} l_i g(\sigma, \sigma_1)}$ to assure that

$$D\left(m_{\mathrm{c}}{}'\right) \leqslant (1+\varepsilon) \sum_{i=1}^{n/k} l_i g\left(\sigma, \sigma_1\right). \tag{20}$$

$$R_a = \frac{1}{\Gamma\left(1 + \sum_{i=a}^{n/k} l_i \Big/ 2\right)} \left(\frac{\pi\left(1+\varepsilon\right)\left(\left(2{\sigma_1}^2 - \sqrt{2\pi}\sigma_1 + 1\right)\frac{\left(2^c+1\right)\left(2^c-1\right)}{12} + \sigma^2\right) \sum_{i=a}^{n/k} l_i}{2^{2c}} \right)^{\sum_{i=a}^{n/k} l_i \Big/ 2} \tag{10}$$

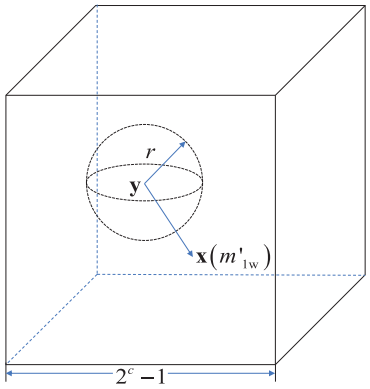

Fig. 3. The relationship between $\mathbf{y}$ and $\mathbf{x}(m'_{1\mathrm{w}})$.

As $\frac{e^{\varepsilon}}{(1+\varepsilon)^{1+\varepsilon}}$ decreases monotonically with respect to ε, it turns out that $\frac{e^{\varepsilon}}{(1+\varepsilon)^{1+\varepsilon}} < 1$. Then, we can obtain that

$$\lim_{\sum_{i=1}^{n/k} l_i g(\sigma,\sigma_1)\to\infty} 1-\left(\frac{e^{\varepsilon}}{(1+\varepsilon)^{1+\varepsilon}}\right)^{\sum_{i=1}^{n/k} l_i g(\sigma,\sigma_1)} = 1. \quad (21)$$

(19) and (21) means that for a large enough $\sum_{i=1}^{n/k} l_i g(\sigma,\sigma_1)$, (20) possess an extremely high probability to be true. Similarly, we can also declare that $D_a(m'_{\mathrm{c}}) \le (1+\varepsilon)\sum_{i=a}^{n/k} l_i g(\sigma,\sigma_1)$ for an appropriate parameter selection of ε and $\sum_{i=a}^{n/k} l_i g(\sigma,\sigma_1)$.

3) Cost Analysis of Wrong Sequences: At last, we analyze the cost of wrong candidate sequences in M'_{w}, which is denoted by $D(m'_{\mathrm{w}})$. The FER of Spinal codes is

$$P_e = \mathbb{P}\left(\exists m'_{\mathrm{w}} : D\left(m'_{\mathrm{w}}\right) \le D\left(m'_{\mathrm{c}}\right)\right). \quad (22)$$

Let $m'_{1\mathrm{w}} = [m'_1, m'_2 \ldots, m'_{n/k}]$ be a member of set $M'_{1\mathrm{w}}$, where $M'_{1\mathrm{w}}$ is defined as

$$M_{1\mathrm{w}}{}' = \left\{ m_{1\mathrm{w}}{}' \middle| m_1{}' \ne m_1 \right\}. \quad (23)$$

Let E_i represent the event that there exists an error in the i^{th} segment m_i. By applying (20) and the union bound of probability, we have

$$\begin{aligned}\mathbb{P}\left(E_1\right) &\le \sum_{m'_{1\mathrm{w}}\in M'_{1\mathrm{w}}} \mathbb{P}\left(D\left(m'_{1\mathrm{w}}\right) \le D\left(m'_{\mathrm{c}}\right)\right) \\ &\le \sum_{m'_{1\mathrm{w}}\in M'_{1\mathrm{w}}} \mathbb{P}\left(D\left(m'_{1\mathrm{w}}\right) \le (1+\varepsilon)\sum_{i=1}^{n/k} l_i g\left(\sigma,\sigma_1\right)\right).\end{aligned} \quad (24)$$

Due to Spinal codes' coding structure which combines a hash function with an RNG, all the coded symbols in $\mathbf{x}(m'_{\mathrm{c}})$ and $\mathbf{x}(m'_{1\mathrm{w}})$ are mapped independently and randomly. Now for the uniform constellation, it is easy to verify that the coded symbol $x_{i,j}(m'_{1\mathrm{w}})$ is independent with $x_{i,j}(m'_c)$ for any $i \ge 1$ and obeys uniform distribution $\mathrm{U}(0, 2^c - 1)$.

The relationship between $\mathbf{y}$ and $\mathbf{x}(m'_{1\mathrm{w}})$ can be intuitively displayed by Fig. 3, where $\mathbf{y}$ is the received matrix, r is related to the approximate upper bound we derived in (24), $\mathbf{x}(m'_{1\mathrm{w}})$ obeys the uniform distribution $\mathrm{U}(0, 2^c - 1)$. Therefore, we can approximate the probability in (24) as follows.

$$\begin{aligned}&\mathbb{P}\left(D\left(m'_{1\mathrm{w}}\right) \le (1+\varepsilon)\, g\left(\sigma,\sigma_1\right)\sum_{i=1}^{n/k} l_i\right) \\ &\approx \frac{V_{\mathrm{b}}\left(\sqrt{(1+\varepsilon)\, g\left(\sigma,\sigma_1\right)\sum_{i=1}^{n/k} l_i}, \sum_{i=1}^{n/k} l_i\right)}{V_{\mathrm{c}}\left(2^c, \sum_{i=1}^{n/k} l_i\right)} \\ &= \frac{1}{\Gamma\left(1+\sum_{i=1}^{n/k} l_i/2\right)}\left(\frac{\pi\,(1+\varepsilon)\, g\left(\sigma,\sigma_1\right)\sum_{i=1}^{n/k} l_i}{2^{2c}}\right)^{\sum_{i=1}^{n/k} l_i/2},\end{aligned} \quad (25)$$

where $V_{\mathrm{b}}(r,n)$ is the volume of an $n-$dimensional ball with radius r and $V_{\mathrm{c}}(l,n)$ is the volume of an $n-$dimensional cube with side length l.

Since the volume of the ball in (25) might be larger than the volume of the cube when $g(\sigma,\sigma_1)$ is large enough, the function $\min(1,\cdot)$ can be applied to modify it as follows.

$$\begin{aligned}\mathbb{P}\left(E_1\right) &\le \sum_{m'_{1\mathrm{w}}\in M'_{1\mathrm{w}}} \mathbb{P}\left(D\left(m'_{1\mathrm{w}}\right) \le (1+\varepsilon)\, g\left(\sigma,\sigma_1\right)\sum_{i=1}^{n/k} l_i\right) \\ &\lessapprox \sum_{m'_{1\mathrm{w}}\in M'_{1\mathrm{w}}} \min\left(1, R_1\right) \\ &= \left|M'_{1\mathrm{w}}\right| \min\left(1, R_1\right),\end{aligned} \quad (26)$$

where $|M'_{1\mathrm{w}}|$ denotes the size of $M'_{1\mathrm{w}}$ with $|M'_{1\mathrm{w}}| = \left(2^k - 1\right)2^{n-k}$ and R_1 is equal to the right hand side of (25).

Furthermore, (26) can also be further modified by $\min(1,\cdot)$.

$$\mathbb{P}\left(E_1\right) \lessapprox \min\left\{1, \left(2^k - 1\right)2^{n-k} \cdot \min\left(1, R_1\right)\right\}. \quad (27)$$

Next, we analyze an approximate upper bound of $\mathbb{P}(E_a|\overline{E}_1,\ldots,\overline{E}_{a-1}), a \ge 2$. Let $m'_{a\mathrm{w}} = [m'_1, m'_2 \ldots, m'_{n/k}]$ be a member of set $M'_{a\mathrm{w}}$, where $M'_{a\mathrm{w}}$ is defined as

$$M_{a\mathrm{w}}{}' = \left\{ m_{a\mathrm{w}}{}' \middle| m'_1 = m_1, \ldots, m'_{a-1} = m_{a-1}, m'_a \ne m_a \right\}. \quad (28)$$

Similarly, it holds that

$$\mathbb{P}(E_a|\overline{E}_1,\ldots,\overline{E}_{a-1}) \le \sum_{m'_{a\mathrm{w}}\in M'_{a\mathrm{w}}} \mathbb{P}\left(D\left(m'_{a\mathrm{w}}\right) \le D\left(m'_{\mathrm{c}}\right)\right). \quad (29)$$

Since $m'_1 = m_1, m'_2 = m_2, \ldots, m'_{a-1} = m_{a-1}, \ldots, m'_a \ne m_a$, we have $x_{i,j}\left(m'_{\mathrm{c}}\right) = x_{i,j}\left(m'_{a\mathrm{w}}\right)$ for any $i < a$.

Then, $\mathbb{P}\left(D\left(m'_{\mathrm{aw}}\right) \leq D\left(m'_{\mathrm{c}}\right)\right)$ can be reduced to

$$\mathbb{P}\left(\sum_{i=a}^{n/k}\sum_{j=1}^{l_i}\left(y_{i,j}-x_{i,j}\left(m'_{\mathrm{aw}}\right)\right)^2 \leq \sum_{i=a}^{n/k}\sum_{j=1}^{l_i}\left(y_{i,j}-x_{i,j}\left(m'_{\mathrm{c}}\right)\right)^2\right). \quad (30)$$

Denote $\sum_{i=a}^{n/k}\sum_{j=1}^{l_i}\left(y_{i,j}-x_{i,j}\left(m'_{\mathrm{aw}}\right)\right)^2$ as $D_a\left(m'_{\mathrm{aw}}\right)$. We obtain that

$$\begin{aligned}
&\mathbb{P}(E_a|\overline{E}_1,\ldots,\overline{E}_{a-1})\\
&\leq \sum_{m'_{\mathrm{aw}}\in M'_{\mathrm{aw}}} \mathbb{P}\left(D\left(m'_{\mathrm{aw}}\right) \leq D\left(m'_{\mathrm{c}}\right)\right)\\
&\overset{(a)}{=} \sum_{m'_{\mathrm{aw}}\in M'_{\mathrm{aw}}} \mathbb{P}\left(D_a\left(m'_{\mathrm{aw}}\right) \leq D_a\left(m'_{\mathrm{c}}\right)\right)\\
&\overset{(b)}{\leq} \sum_{m'_{\mathrm{aw}}\in M'_{\mathrm{aw}}} \mathbb{P}\left(D_a\left(m'_{\mathrm{aw}}\right) \leq (1+\varepsilon)\, g\left(\sigma,\sigma_1\right)\sum_{i=a}^{n/k} l_i\right)\\
&\overset{(c)}{\approx} \sum_{m'_{\mathrm{aw}}\in M'_{\mathrm{aw}}} \frac{V_{\mathrm{b}}\left(\sqrt{(1+\varepsilon)\, g\left(\sigma,\sigma_1\right)\sum_{i=a}^{n/k} l_i}, \sum_{i=a}^{n/k} l_i\right)}{V_{\mathrm{c}}\left(2^c, \sum_{i=a}^{n/k} l_i\right)}\\
&\leq \left|M'_{\mathrm{aw}}\right| \min\left(1, R_a\right)\\
&= \left(2^k-1\right) 2^{n-ak} \min\left(1, R_a\right)\\
&\leq \min\left\{1, \left(2^k-1\right) 2^{n-ak}\cdot \min\left(1, R_a\right)\right\}, \quad (31)
\end{aligned}$$

where R_a is calculated using

$$\begin{aligned}
R_a &= \frac{V_{\mathrm{b}}\left(\sqrt{(1+\varepsilon)\, g\left(\sigma,\sigma_1\right)\sum_{i=a}^{n/k} l_i}, \sum_{i=a}^{n/k} l_i\right)}{V_{\mathrm{c}}\left(2^c, \sum_{i=a}^{n/k} l_i\right)}\\
&= \frac{1}{\Gamma\left(1+\sum_{i=a}^{n/k} l_i/2\right)}\left(\frac{\pi\,(1+\varepsilon)\, g\left(\sigma,\sigma_1\right)\sum_{i=a}^{n/k} l_i}{2^{2c}}\right)^{\sum_{i=a}^{n/k} l_i/2}. \quad (32)
\end{aligned}$$

In (31), (a) is given by (30), (b) derives from the chernoff bound, and (c) can be obtained similarly as approximation (25) does.

Finally, the FER of Spinal codes, i.e., P_e, can be expressed as follows.

$$\begin{aligned}
P_e &= \mathbb{P}\left(E_1 \cup E_2 \cup \cdots \cup E_{n/k}\right)\\
&= 1-\prod_{a=1}^{n/k}\mathbb{P}\left(\bar{E}_a|\bar{E}_1,\cdots,\bar{E}_{a-1}\right). \quad (33)
\end{aligned}$$

Let $\epsilon_a = \min\left\{1, \left(2^k-1\right)2^{n-ak}\cdot\min\left(1, R_i\right)\right\}$. By adopting (27) and (31), it turns out that

$$P_e \lessapprox 1-\prod_{i=1}^{n/k}(1-\epsilon_a). \quad (34)$$

At last, the proof of Theorem 1 is finished. □

Now that we have completed the derivation of FER upper bound for Spinal codes over the Rayleigh fading channel. In the process of derivation, we assume that $r_{i,j}$ is i.i.d and obeys Rayleigh distribution. In fact, we can popularize the above results only by replacing the distribution of $r_{i,j}$.

For example, if $r_{i,j}$ is a constant and $r_{i,j}=1$, the channel turns into an AWGN channel and we can derive the upper bound for Spinal codes over the AWGN channel by simply recalculating (16). Replace $g\left(\sigma,\sigma_1\right)$ with σ^2, Theorem 2 can be obtained.

Theorem 2 FER Upper Bound for Spinal Codes Over the AWGN Channel: Consider Spinal codes with message length n, segmentation parameter k and modulation parameter c transmitted over an AWGN channel with noise variance σ^2, then the FER under ML decoding can be upper bounded by

$$P_e \lessapprox 1-\prod_{a=1}^{n/k}(1-\epsilon_a), \quad (35)$$

with

$$\epsilon_a = \min\left\{1, \left(2^k-1\right)2^{n-ak}\cdot\min\left(1, R_a\right)\right\}, \quad (36)$$

where

$$R_a = \frac{1}{\Gamma\left(1+\sum_{i=a}^{n/k} l_i \Big/ 2\right)}\left(\frac{\pi\,(1+\varepsilon)\,\sigma^2\sum_{i=a}^{n/k} l_i}{2^{2c}}\right)^{\sum_{i=a}^{n/k} l_i \Big/ 2}. \quad (37)$$

C. Simulation Results

The simulation is carried out with ML decoding. We set the parameter n as short as 8 due to its exponential complexity. (This makes the ML-decoding-based simulation realizable without affecting the verification of the non-asymptotic FER upper bound), other related parameters are set as follows: segmentation parameter $k=2$, hash coefficient $v=32$, Rayleigh fading coefficient $\sigma_1=0.7$, the number of transmission passes $Pass=15$ and modulation parameter $c=8$. Through simulations, we find that $\varepsilon=1$ is a good choice to hold the upper bound. As a result, in this paper we choose $\varepsilon=1$ to characterize the approximate FER upper bound.

Fig. 4 (a) shows the corresponding comparison over the AWGN channel. The simulation is carried out with ML decoding with $n=8$, $k=2$, $v=32$, $Pass=8$ and $c=8$. From Fig. 4, we can see that the derived upper bound fits the simulation FER well and approaches the simulation FER as

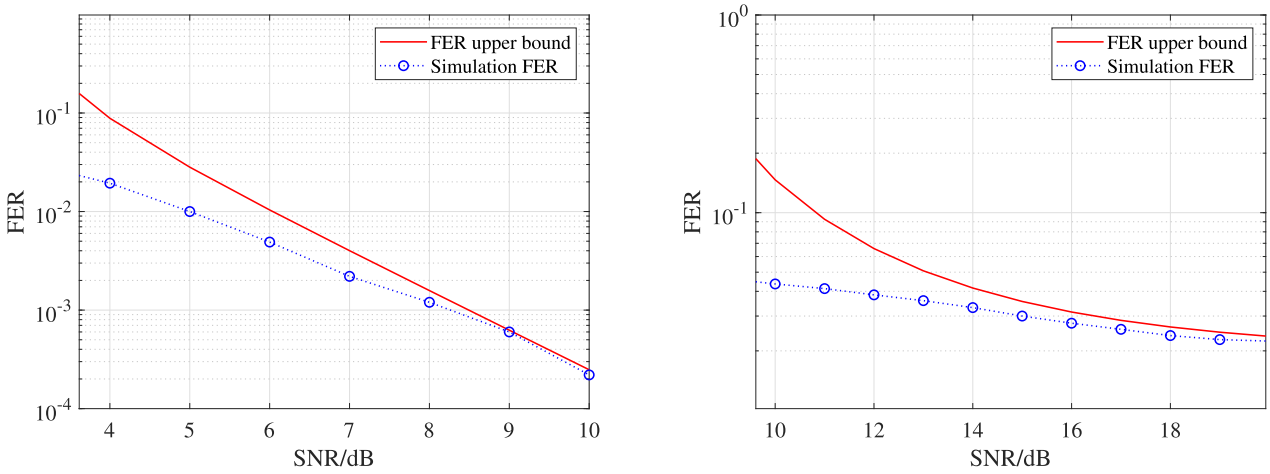

(a) FER over the AWGN Channel.

(b) FER over the the Rayleigh fading channel with $\sigma_1 = 0.7$.

Fig. 4. Comparison between simulation results and FER upper bounds with $n = 8$, $v = 32$, $k = 2$, $c = 8$ and $\varepsilon = 1$.

SNR increases. These simulation results verify the correctness of Theorem 1 and Theorem 2.

From Fig. 4 (b), we can observe that the FER performance of Spinal codes is not ideal over the Rayleigh fading channel. To improve the FER performance of Spinal codes over the Rayleigh fading channel, we propose a new structural design called self-concatenation Spinal codes. The specific form of the structure, the reason we propose this structure, and the detailed theoretical analysis of our proposed structure will be shown in the next section.

IV. Self-Concatenation Spinal Codes

By investigating the structure of Spinal codes, we can find that a coded symbol $x_{a,j}$ is only related to the segmentation sequence m_i with $i \leq a$. On the contrary, for a segmentation sequence m_a, the coded symbols that relate to it are $x_{i,j}$ with $i \geq a$. For ML decoding, if there is a candidate sequence $M' = (m'_1, m'_2 \ldots, m'_{n/k})$ which is inconsistent with the correct sequence $M = (m_1, m_2 \ldots, m_{n/k})$ from the a^{th} segmentation sequence with $m_1 = m'_1, m_2 = m'_2, \ldots, m'_a \neq m_a$, we have $x_{i,j}(M) = x_{i,j}(M')$ for $i < a$, and $x_{i,j}(M)$ are independent with $x_{i,j}(M')$ for $i \geq a$. In fact, the independence between $x_{i,j}(M)$ and $x_{i,j}(M')$ will significantly increase the Euclidean distance between them. Then, considering that the decoder tends to choose the best matching sequence of the encoding vector that is closest to the received symbol in Euclidean distance, it can be inferred that when an error occurs, the number of independent symbols between $x_{i,j}(M)$ and $x_{i,j}(M')$ determines the error correction ability of the system.

Specifically, in the derivation process of FER analysis, when an error occurs at m_a, the number of encoded symbols $x_{i,j}(M')$ that are independent with $x_{i,j}(M)$ can be calculated by $\sum_{i=a}^{n/k} l_i$. From (9) and (10), it can be proved that ϵ_a is monotone decreasing with respect to $\sum_{i=a}^{n/k} l_i$. Therefore, our goal of structural design of Spinal codes is to further increase the number of independent symbols $\sum_{i=a}^{n/k} l_i$ when an error occurs.

A. The Encoding Structure of Self-Concatenation Spinal Codes

The encoding structure of self-concatenation Spinal codes is shown in Fig. 5. The coding process of self-concatenation Spinal codes can be divided into 5 steps:

Step 1: An n-bit message M is divided into n/k k-bit segments. The segment is denoted by m_i, where $i \in \{1, 2, \ldots, n/k\}$.

Step 2: The encoder calls the hash function n/k times to generate the hash state value $s_{n/k}$.

Step 3: The hash state value $s_{n/k}$ serves as an initial state of the original Spinal codes to iteratively generate the hash state value.

Step 4: The v-bit hash state is input to the RNG as a seed to generate pseudo-random c-bit symbols denoted by $x_{i,j}$.

Step 5: The encoder maps the c-bit symbols to a channel input set to fit the channel characteristics.

The ML decoding process of self-concatenation Spinal codes is the same as original Spinal codes, which can be expressed in (4).

B. FER Analysis of Self-Concatenation Spinal Codes

The design of self-concatenation Spinal codes is inspired by the FER analysis of Spinal codes over the Rayleigh fading channel. In this subsection, we derive an approximate FER upper bound for self-concatenation Spinal codes. The rationality and superiority of self-concatenation Spinal codes are explained theoretically in this subsection.

Theorem 3 FER Upper Bound for Self-Concatenation Spinal Codes Over the Rayleigh Fading Channel: Consider Spinal codes with message length n, segmentation parameter k and modulation parameter c transmitted over an AWGN channel with noise variance σ^2, and Rayleigh parameter σ_1, then the FER under ML decoding can be upper bounded by

$$P_e \lessapprox 1 - \prod_{i=1}^{n/k} (1 - \epsilon_i), \tag{38}$$

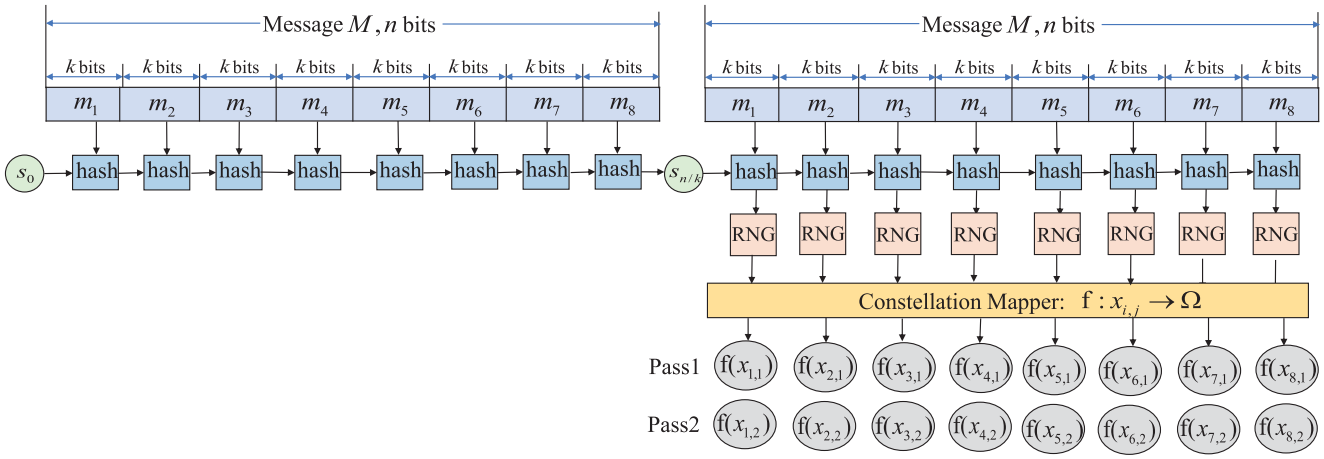

Fig. 5. The encoding process of self-concatenation Spinal codes.

with

$$\epsilon_a = \min\left\{1, \left(2^k - 1\right) 2^{n-ak} \cdot \min\left(1, R\right)\right\}, \tag{39}$$

where R can be calculated by (40), shown at the bottom of the page.

The idea of the proof of Theorem 3 is slightly similar to the proof of Theorem 1, and thus we give the detailed derivation in Appendix A.

Remark 1: Compare Theorem 3 with Theorem 1, we can see that the only difference of the FER upper bounds between the original Spinal codes and the proposed self-concatenation Spinal codes is that, for the original Spinal codes, ϵ_a is with respect to $\sum_{i=a}^{n/k} l_i$; For the self-concatenation Spinal codes, ϵ_a is with respect to $\sum_{i=1}^{n/k} l_i$. Consider that ϵ_a is monotone decreasing with respect to $\sum_{i=a}^{n/k} l_i$ or $\sum_{i=1}^{n/k} l_i$, we can qualitatively conclude that the FER of self-concatenation Spinal codes is lower than that of original Spinal codes. Corresponding simulation results will be shown in Section VI.

V. Parallel Self-Concatenation Spinal Codes

It can be known from the theoretical analysis and simulation results that the FER performance of the proposed self-concatenation Spinal is outstanding. (even when the length of message sequence n is as short as 8). However, due to the particularity of coding structure, ML decoding without pruning seems to be the only decoding method, which may result in exponential complexity with regard to n. As a result, we can only conclude that self-concatenation Spinal codes is practical with outstanding FER performance when the length of message sequence is short, but how to utilize it in the case of long message sequence length remains a problem. In this section, the concept of parallel structure is proposed to solve this problem. By parallel self-concatenating, not only the encoding and decoding throughput of Spinal codes is improved, but also the FER is reduced.

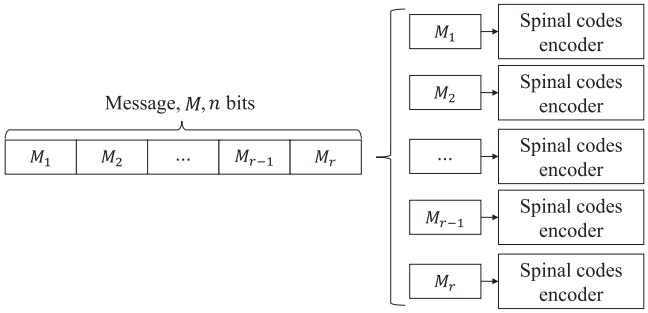

Fig. 6. The encoding structure of parallel Spinal codes.

A. Parallel Spinal Codes

In this subsection, we begin with introducing the parallel structure of Spinal codes, and then analyze the advantages and disadvantages of it.

The encoding structure of parallel Spinal codes is shown in Fig. 6, which can be divided into two steps: 1) A message sequence M is uniformly divided into r parallel sub-sequences to; 2) These sub-sequences are fed into Spinal codes encoders respectively to generate pseudo-random code words.

The advantage of the parallel operation is mainly in the aspect of decoding throughput. Let's take $n = 32$,

$$R = \frac{1}{\Gamma\left(1 + \sum_{i=1}^{n/k} l_i \Big/ 2\right)} \left(\frac{\pi\left(1+\varepsilon\right)\left(\left(2{\sigma_1}^2 - \sqrt{2\pi}\sigma_1 + 1\right)\frac{\left(2^c+1\right)\left(2^c-1\right)}{12} + \sigma^2\right)\sum_{i=1}^{n/k} l_i}{2^{2c}} \right)^{\sum_{i=1}^{n/k} l_i \Big/ 2} \tag{40}$$

$r = 4$ as an example. For a message sequence with message length $n = 32$, if ML decoding algorithm is used, the number of candidate sequences at the decoding end is 2^{32}, and thus the decoding process needs 2^{32} cost calculations. Nevertheless, if the sequence is divided into four 8-bit sub-sequences and each sub-sequence adopts ML decoding algorithm, the number of candidate sequences of each sub-sequence is 2^8. For the decoding of the complete message sequence, the decoding process needs $4 \times 2^8 = 2^{10}$ cost calculations. Compared with original Spinal codes, the decoding throughput of the parallel structure increases by nearly 2^{22} times. As a result, we can conclude that the parallel structure can significantly improve the decoding throughput of Spinal codes.

However, the improvement of decoding complexity sacrifices the FER performance. In [20], Gallager derives that under ML decoding, the average error probability of a random code is

$$P_e \leq 2^{-nRE(R)}, \tag{41}$$

where n is the length of the message sequence, R is the rate of the random code, and $E_r(R)$ is with respect to R. From (36), it turns out that the average error probability upper bound of a fixed-rate random code decreases exponentially with respect to the length of the message sequence n. The parallel structure divides the long message sequence into several short subsequences, and thus results in the rise of the FER upper bound. To mathematically elaborate it, we define that $P_{e-\mathrm{OS}}$ is the FER of original Spinal codes, $P_{e-\mathrm{PS}}$ is the FER of parallel Spinal codes and P_e is the FER of the divided subsequences. For parallel Spinal codes with r parallel subsequences, the correct decoding of the message sequence is equivalent to the correct decoding of all the parallel subsequences. Therefore, we have

$$P_{e-\mathrm{PS}} = 1 - (1 - P_e)^4. \tag{42}$$

Due to (36), we can obtain that $P_{e-\mathrm{OS}} < P_e$. Thus we obtain that

$$\begin{aligned} P_{e-\mathrm{OS}} &< 1 - (1 - P_{e-\mathrm{OS}})^4 \\ &< 1 - (1 - P_e)^4 \\ &= P_{e-\mathrm{PS}}. \end{aligned} \tag{43}$$

To conclude, the parallel structure can significantly increase the decoding throughput of Spinal codes, but this decoding throughput improvement is at the cost of sacrificing the FER performance.

B. Parallel Self-Concatenation Spinal Codes

Considering the excellent FER performance of self-concatenation Spinal codes, we combine the parallel structure with the self-concatenation structure: the parallel structure improves the decoding throughput under ML decoding; the self-concatenation structure compensates the FER loss resulted by the parallel structure. The basic structure of self-concatenation Spinal codes is shown in Fig. 7.

Here, the general idea of error probability analysis corresponding to parallel self-concatenation Spinal codes is also given. Denote P'_e as the FER of the sub-sequences of self-concatenation Spinal codes, $P_{e-\mathrm{PSCS}}$ is the FER of parallel self-concatenation Spinal codes. For parallel Spinal codes with r sub-sequences, the correct decoding of the message sequence is equivalent to the correct decoding of all the four sub-sequences. Therefore, we can calculate $P_{e-\mathrm{PSCS}}$ by

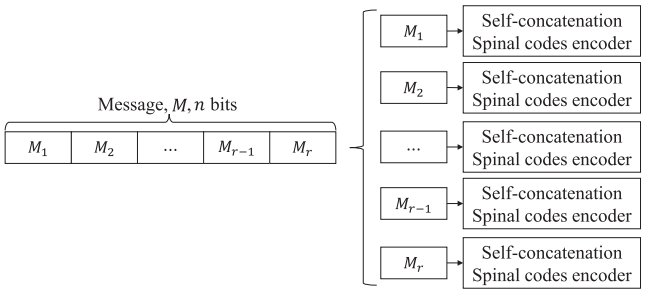

Fig. 7. The encoding structure of parallel self-concatenation Spinal codes.

$$P_{e-\mathrm{PSCS}} = 1 - (1 - P'_e)^4, \tag{44}$$

where P'_e can be upper bounded by Theorem 3.

C. Qualitative Analysis of Performance

1) FER Comparison: From (38), i.e., $P_{e-\mathrm{OS}} < P_{e-\mathrm{PS}}$, we can conclude that the paralleling operation will raise up the FER of Spinal codes. However, self-concatenation Spinal codes takes an advantage over original Spinal codes in FER with $P'_e < P_e$. After the parallel operation, it holds that $P_{e-PSCS} = 1 - (1 - P'_e)^r$ and $P_{e-PS} = 1 - (1 - P_e)^r$. Since $P'_e < P_e$, we can obtain that $P_{e-PSCS} < P_{e-PS}$. As a result, we conclude that the self-concatenation structure could compensate for the FER loss resulted from the parallel structure.

2) Complexity Analysis: For Spinal codes using ML decoding algorithm, the average decoding time can be succinctly expressed as $O = NC$, where N denotes the number of cost calculations and C is the average time of each cost calculation. For original Spinal codes, we have $O_{\mathrm{OS}} = 2^n C_{\mathrm{OS}}$; For parallel Spinal codes, it holds that $O_{\mathrm{PS}} = r2^{n/r} C_{\mathrm{PS}}$; For parallel self-concatenation Spinal codes, we have $O_{\mathrm{SCPS}} = r2^{n/r} C_{\mathrm{SCPS}}$. As the coding structure of self-concatenation Spinal codes is more complicated than that of original Spinal codes, we have $C_{\mathrm{SCPS}} > C_{\mathrm{PS}}$ and thus it is evident to hold that $O_{\mathrm{SCPS}} > O_{\mathrm{PS}}$. We can also obtain that $\frac{O_{\mathrm{OS}}}{O_{\mathrm{SCPS}}} = \frac{2^n C_{\mathrm{OS}}}{r2^{n/r} C_{\mathrm{PS}}}$. Since $\frac{2^n}{r2^{n/r}} = \mathrm{O}\left(\left(2^{1-\frac{1}{r}}\right)^n\right)$ and $\frac{C_{\mathrm{OS}}}{C_{\mathrm{PS}}} = \mathrm{O}(1)$, we can infer that $O_{\mathrm{OS}} > O_{\mathrm{SCPS}}$ is true for most of the choices of message length n. (More detailed and visual results are shown through Monte Carlo simulations in Section VI.)

VI. Simulation Results

Fig. 8 demonstrates the comparison of FER performance between self-concatenation Spinal codes and original Spinal codes. The simulations are carried out with ML decoding rule. We set the length of message sequence n as short as 8, other related parameters are set as follows: segmentation

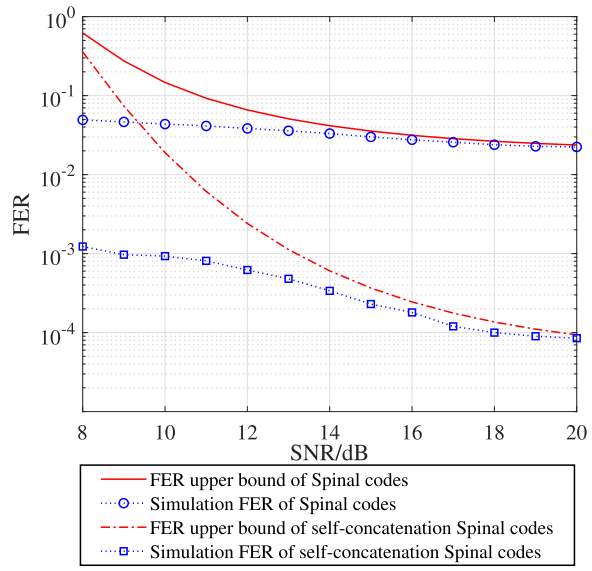

Fig. 8. FER performance comparison and upper bounds over the Rayleigh fading channel with $n = 8$, $k = 2$, $c = 8$, $\sigma_1 = 0.7$ and $\varepsilon = 1$.

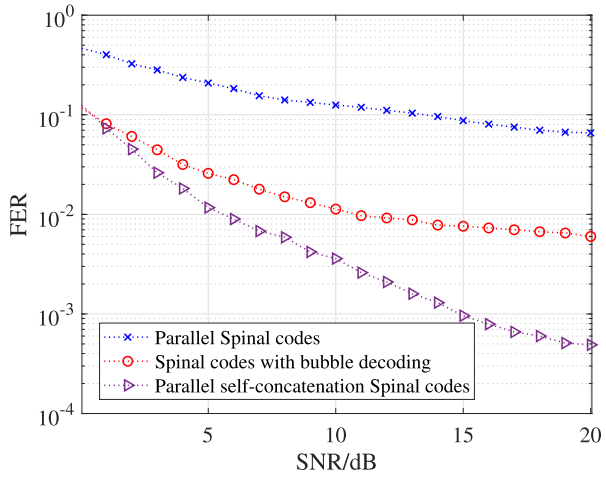

Fig. 9. FER performance comparison over the Rayleigh fading channel with $\sigma_1 = 0.7$.

parameter $k = 2$, Rayleigh coefficient $\sigma_1 = 0.7$, the number of transmission passes $Pass = 15$, modulation parameter $c = 8$.

From Fig. 8, we can see that by introducing the self-concatenation structure, the FER of Spinal codes over Rayleigh channels significantly reduces. Besides, Fig. 8 also confirms the effectiveness of the FER upper bound of self-concatenation Spinal codes. The derived upper bounds fit better with the simulation results as SNR increases. The gap at the low SNR regime is mainly due to corresponding looseness of Eq. (25), where the volume of the ball may be bigger than the volume of the cube when the noise variance is too large.

Fig. 9 shows the comparison of FER performance among the proposed parallel self-concatenation Spinal codes, the parallel Spinal codes, and the original Spinal codes with bubble decoding. For the parallel self-concatenation Spinal codes and parallel Spinal codes, the message length is $n = 24$, which

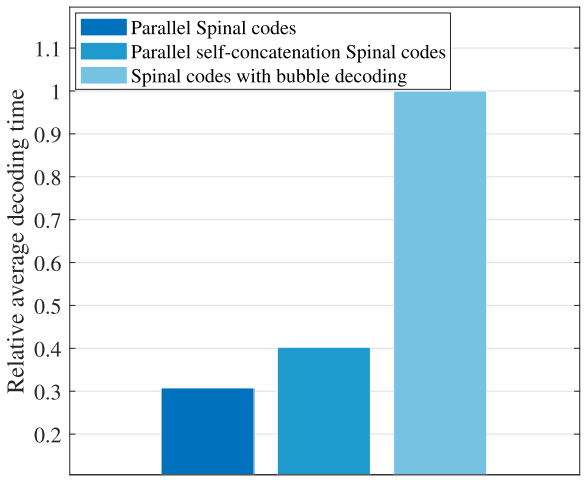

Fig. 10. Normalized decoding time comparison among different coding-decoding pairs.

are divided into 3 sub-sequences. The segmentation parameter k is set as $k = 2$ for the sub-sequence and the number of transmission passes is set as $Pass = 15$. For the original Spinal codes with bubble decoding, we set the length of the message sequence n as 24, other related parameters are set as follows: segmentation parameter $k = 4$, the number of transmission passes $Pass = 30$, bubble pruning parameter $B = 64$. The simulations are both carried out under the same fixed rate, the same Rayleigh coefficient $\sigma_1 = 0.7$, and the same modulation parameter $c = 8$.

Fig. 10 gives the average normalized decoding time of different 'transmission scheme - decoding algorithm' pairs. It can be seen that the decoding time of parallel self-concatenation Spinal codes takes a tremendous advantage over the parallel Spinal codes with bubble decoding. Although the decoding time of parallel self-concatenation Spinal codes is slightly higher than the parallel Spinal codes with ML decoding due to its special coding structure, considering the poor FER performance of parallel Spinal codes, the parallel self-concatenation Spinal codes holds greater practicability.

From Fig. 9 and Fig. 10, we can conclude that by parallel self-concatenating, both the FER performance and the decoding throughput are promoted evidently compared with the original Spinal codes with bubble decoding, which gives rise to the extensive application value of parallel self-concatenation Spinal codes.

VII. Conclusion and Future Works

In this paper, we aim to solve the problem of poor FER performance and insufficient decoding throughput of Spinal codes over the Rayleigh fading channel. We begin with analyzing the non-asymptotic FER performance of Spinal codes over the Rayleigh fading channel. Also, inspired by the FER analysis, we propose a self-concatenation structure to ameliorate its poor FER performance. The proposed self-concatenation Spinal codes can be applied in the scenario wherein the message sequence is very short. For a longer sequence that is not suitable for ML decoding, the parallel structure is introduced

to improve the decoding throughput of self-concatenation Spinal codes. By parallel self-concatenating, both the FER performance and the decoding throughput are promoted evidently compared with the original Spinal codes with bubble decoding. We hope that this work will stimulate further research in the application of high-efficiency Spinal-codes-based techniques.

The investigation in this paper also leaves some open challenges and issues for future research. We briefly discuss some of them in the following. First, the FER analysis in this paper is based on the optimal ML decoding algorithm over the Rayleigh fading channel. For Spinal codes, the error probability analysis of some practical low-complexity decoding algorithms, such as the bubble decoding algorithm and the FSD decoding algorithm, is still to be derived. Furthermore, we believe that designing a customized practical decoding algorithm for the proposed self-concatenation structure will be of great potential in the future.

APPENDIX A
PROOF OF THEOREM 3

The proof of Theorem 3 can be also divided into three steps: **1) Candidate Sequences Classification**; **2) Cost Analysis of Correct Sequences**; **3) Cost Analysis of Wrong Sequences**. The main difference with the proof of Theorem 2 occurs in the third step. Therefore, we elaborate **3) Cost Analysis of Wrong Sequences** here.

Proof: **3) Cost Analysis of Wrong Sequences.**, Similarly, The FER of Spinal codes is

$$P_e = \mathbb{P}\left(\exists m'_{\mathrm{w}} : D\left(m'_{\mathrm{w}}\right) \leq D\left(m'_{\mathrm{c}}\right)\right). \tag{45}$$

Let $M'_{1\mathrm{w}} = [m'_1, m'_2 \ldots, m'_{n/k}]$ denote the set of wrong sequences with $m'_1 \neq m_1$, $m'_{1\mathrm{w}} \in M'_{1\mathrm{w}}$. Let E_i represent the event that there exists an error in the i^{th} segment. By applying the union bound of probability, we have

$$\mathbb{P}\left(E_1\right) \leq \sum_{m'_{1\mathrm{w}}} \mathbb{P}\left(D\left(m'_{1\mathrm{w}}\right) \leq D\left(m'_{\mathrm{c}}\right)\right). \tag{46}$$

By similarly utilizing the chernoff bound, it turns out that

$$\mathbb{P}\left(E_1\right) \leq \sum_{m'_{1\mathrm{w}}} \mathbb{P}\left(D\left(m'_{1\mathrm{w}}\right) \leq (1+\varepsilon)\, g\left(\sigma, \sigma_1\right) \sum_{i=1}^{n/k} l_i\right). \tag{47}$$

The probability in (47) can be approximated as follows:

$$\begin{aligned}
&\mathbb{P}\left(D\left(m'_{1\mathrm{w}}\right) \leq (1+\varepsilon)\, g\left(\sigma, \sigma_1\right) \sum_{i=1}^{n/k} l_i\right) \\
&\approx \frac{V_{\mathrm{b}}\left(\sqrt{(1+\varepsilon)\, g\left(\sigma, \sigma_1\right) \sum_{i=1}^{n/k} l_i}, \sum_{i=1}^{n/k} l_i\right)}{V_{\mathrm{c}}\left(2^c, \sum_{i=1}^{n/k} l_i\right)} \\
&= \frac{1}{\Gamma\left(1 + \sum_{i=1}^{n/k} l_i/2\right)} \left(\frac{\pi\,(1+\varepsilon)\, g\left(\sigma, \sigma_1\right) \sum_{i=1}^{n/k} l_i}{2^{2c}}\right)^{\sum_{i=1}^{n/k} l_i/2},
\end{aligned} \tag{48}$$

where $V_{\mathrm{b}}\left(r, n\right)$ is the volume of an $n-$dimensional ball with radius r and $V_{\mathrm{c}}\left(l, n\right)$ is the volume of an $n-$dimensional cube with side length l.

Since the volume of the ball in (48) might be larger than the volume of the cube when $g\left(\sigma, \sigma_1\right)$ is large enough, the function $\min\left(1, \cdot\right)$ can be applied to modify it as follows.

$$\begin{aligned}
\mathbb{P}\left(E_1\right) &\leq \sum_{m'_{1\mathrm{w}} \in M'_{1\mathrm{w}}} \mathbb{P}\left(D\left(m'_{1\mathrm{w}}\right) \leq (1+\varepsilon)\, g\left(\sigma, \sigma_1\right) \sum_{i=1}^{n/k} l_i\right) \\
&\lessapprox \sum_{m'_{1\mathrm{w}} \in M'_{1\mathrm{w}}} \min\left(1, R_1\right) \\
&= |M'_{1\mathrm{w}}| \min\left(1, R_1\right),
\end{aligned} \tag{49}$$

where $|M'_{1\mathrm{w}}|$ denotes the size of $M'_{1\mathrm{w}}$ with $|M'_{1\mathrm{w}}| = \left(2^k - 1\right) 2^{n-k}$ and R_1 is equal to the right hand side of (43). Furthermore, (49) can also be further modified by $\min\left(1, \cdot\right)$.

$$\mathbb{P}\left(E_1\right) \lessapprox \min\left\{1, \left(2^k - 1\right) 2^{n-k} \cdot \min\left(1, R_1\right)\right\}. \tag{50}$$

Next, we analyze an approximate upper bound of $\mathbb{P}(E_a|\overline{E}_1, \ldots, \overline{E}_{a-1}), a \geq 2$. Let $M'_{a\mathrm{w}} = [m'_1, m'_2 \ldots, m'_{n/k}]$ denote the set of wrong sequences with $m'_1 = m_1, m'_2 = m_2, \ldots, m'_{a-1} = m_{a-1}, \ldots, m'_a \neq m_a$. Let $m'_{a\mathrm{w}} \in M'_{a\mathrm{w}}$. Similarly, It holds that

$$\mathbb{P}(E_a|\overline{E}_1, \ldots, \overline{E}_{a-1}) \leq \sum_{m'_{a\mathrm{w}} \in M'_{a\mathrm{w}}} \mathbb{P}\left(D\left(m'_{a\mathrm{w}}\right) \leq D\left(m'_{\mathrm{c}}\right)\right). \tag{51}$$

Due to self-concatenation structure of Spinal codes, though $m'_1 = m_1, m'_2 = m_2, \ldots, m'_{a-1} = m_{a-1}, \ldots, m'_a \neq m_a$, we cannot conclude that $x_{i,j}\left(m'_{\mathrm{c}}\right) = x_{i,j}\left(m'_{a\mathrm{w}}\right)$ for any $i < a$ here (the main difference with that in the proof of Theorem 2). The reason is that for any $1 \leq a \leq n/k$, the error occurs at m_a will result in a different hash state at $s_{n/k}$. Since $s_{n/k}$ serves as an initial hash state for generating all coded symbols $x_{i,j}$ with $1 \leq i \leq n/k$ for self-concatenation Spinal codes, we can obtain that instead of $x_{i,j}\left(m'_{\mathrm{c}}\right) = x_{i,j}\left(m'_{a\mathrm{w}}\right)$ for any $i < a$, all the coded symbols in $\mathbf{x}(m'_{\mathrm{c}})$ and $\mathbf{x}(m'_{1\mathrm{w}})$ are mapped independently and randomly for any $1 \leq a \leq n/k$. Therefore, it holds that

$$\begin{aligned}
&\mathbb{P}(E_a|\overline{E}_1, \ldots, \overline{E}_{a-1}) \\
&\leq \sum_{m'_{a\mathrm{w}} \in M'_{a\mathrm{w}}} \mathbb{P}\left(D\left(m'_{a\mathrm{w}}\right) \leq D\left(m'_{\mathrm{c}}\right)\right) \\
&\leq \sum_{m'_{a\mathrm{w}} \in M'_{a\mathrm{w}}} \mathbb{P}\left(D\left(m'_{a\mathrm{w}}\right) \leq (1+\varepsilon)\, g\left(\sigma, \sigma_1\right) \sum_{i=1}^{n/k} l_i\right)
\end{aligned}$$

$$\approx \sum_{m'_{\mathrm{aw}} \in M'_{\mathrm{aw}}} \frac{V_{\mathrm{b}}\left(\sqrt{(1+\varepsilon)\, g\left(\sigma, \sigma_1\right) \sum_{i=1}^{n/k} l_i}, \sum_{i=1}^{n/k} l_i\right)}{V_{\mathrm{c}}\left(2^c, \sum_{i=1}^{n/k} l_i\right)}$$
$$\leq \left|M'_{\mathrm{aw}}\right| \min\left(1, R\right)$$
$$= \left(2^k - 1\right) 2^{n-ak} \min\left(1, R\right)$$
$$\leq \min\left\{1, \left(2^k - 1\right) 2^{n-ak} \cdot \min\left(1, R\right)\right\}. \quad (52)$$

where R is calculated using

$$R = \frac{V_{\mathrm{b}}\left(\sqrt{g\left(\sigma, \sigma_1\right) \sum_{i=1}^{n/k} l_i}, \sum_{i=1}^{n/k} l_i\right)}{V_{\mathrm{c}}\left(2^c, \sum_{i=1}^{n/k} l_i\right)}$$
$$= \frac{1}{\Gamma\left(1 + \sum_{i=1}^{n/k} l_i/2\right)} \left(\frac{\pi g\left(\sigma, \sigma_1\right) \sum_{i=1}^{n/k} l_i}{2^{2c}}\right)^{\sum_{i=1}^{n/k} l_i/2}. \quad (53)$$

Note that $R = R_1$, let $\epsilon_a = \min\left\{1, \left(2^k - 1\right) 2^{n-ak} \cdot \min\left(1, R\right)\right\}$. By adopting (50) and (52), it turns out that

$$P_e \lessapprox 1 - \prod_{a=1}^{n/k} (1 - \epsilon_a). \quad (54)$$

At last, the proof of Theorem 3 is finished. □

ACKNOWLEDGMENT

The authors would like to thank all the anonymous reviewers that have commented on the past versions of this article, for providing them a lot of valuable suggestions that help them significantly improve the manuscript.

REFERENCES

[1] J. Perry, H. Balakrishnan, and D. Shah, "Rateless spinal codes," in *Proc. ACM HotNets*, 2011, pp. 1–6.
[2] J. Perry, P. A. Iannucci, K. E. Fleming, H. Balakrishnan, and D. Shah, "Spinal codes," in *Proc. ACM SIGCOMM Comput. Commun. Rev.*, vol. 42, no. 4, pp. 49–60, Aug. 2012.
[3] H. Balakrishnan, P. Iannucci, J. Perry, and D. Shah, "De-randomizing Shannon: The design and analysis of a capacity-achieving rateless code," *CoRR*, vol. abs/1206.0418, pp. 1–19, Jun. 2012.
[4] M. Luby, "LT codes," in *Proc. 43rd Annu. IEEE Symp. Found. Comput. Sci.*, Nov. 2002, p. 271.
[5] R. Karp, M. Luby, and A. Shokrollahi, "Finite length analysis of LT codes," in *Proc. Int. Symp. Inf. Theory*, Jun. 2005, p. 39.
[6] A. Shokrollahi, "Raptor codes," *IEEE Trans. Inf. Theory*, vol. 52, no. 6, pp. 2551–2567, Jun. 2006.
[7] G. Joshi, J. B. Rhim, J. Sun, and D. Wang, "Fountain codes," in *Proc. IEEE Global Telecommun. Conf.*, Oct. 2010, pp. 7–12.
[8] K. Zhang, X. Ma, S. Zhao, B. Bai, and X. Zhang, "A new ensemble of rate-compatible LDPC codes," in *Proc. IEEE Int. Symp. Inf. Theory Process.*, Cambridge, MA, USA, 2012, pp. 2536–2540.
[9] M. Zhu, Y. Wei, B. Bai, and X. Ma, "Precoded kite codes for the AWGN channel," in *Proc. Int. Conf. Wireless Commun. Signal Process.*, Hangzhou, China, Oct. 2013, pp. 1–6.
[10] N. Bonello, R. Zhang, S. Chen, and L. Hanzo, "Reconfigurable rateless codes," *IEEE Trans. Wireless Commun.*, vol. 8, no. 11, pp. 5592–5600, Nov. 2009.
[11] M. Shirvanimoghaddam, Y. Li, and B. Vucetic, "Near-capacity adaptive analog fountain codes for wireless channels," *IEEE Commun. Lett.*, vol. 17, no. 12, pp. 2241–2244, Dec. 2013.
[12] R. Rafie Borujeny and M. Ardakani, "A new class of rateless codes based on Reed–Solomon codes," *IEEE Trans. Commun.*, vol. 64, no. 1, pp. 49–58, Jan. 2016.
[13] X. Yu, Y. Li, W. Yang, and Y. Sun, "Design and analysis of unequal error protection rateless spinal codes," *IEEE Trans. Commun.*, vol. 64, no. 11, pp. 4461–4473, Nov. 2016.
[14] A. Li, S. Wu, Y. Wang, J. Jiao, and Q. Zhang, "Spinal codes over BSC: Error probability analysis and the puncturing design," in *Proc. IEEE 91st Veh. Technol. Conf.*, Antwerp, Belgium, Oct. 2020, pp. 1–5.
[15] F. Jelinek, "Fast sequential decoding algorithm using a stack," *IBM J. Res. Develop.*, vol. 13, no. 6, pp. 675–685, Nov. 1969.
[16] S. Xu, S. Wu, J. Luo, J. Jiao, and Q. Zhang, "Low complexity decoding for spinal codes: Sliding feedback decoding," in *Proc. IEEE 86th Veh. Technol. Conf. (VTC-Fall)*, Toronto, ON, USA, Jan. 2017, pp. 1–5, 2017.
[17] Y. Hu, R. Liu, H. Bian, and D. Lyu, "Design and analysis of a low-complexity decoding algorithm for spinal codes," *IEEE Trans. Veh. Technol.*, vol. 68, no. 5, pp. 4667–4679, May 2019.
[18] Y. Li, J. Wu, B. Tan, M. Wang, and W. Zhang, "Compressive spinal codes," *IEEE Trans. Veh. Technol.*, vol. 68, no. 12, pp. 11944–11954, Dec. 2019.
[19] W. Yang, Y. Li, X. Yu, and J. Li, "A low complexity sequential decoding algorithm for rateless spinal codes," *IEEE Commun. Lett.*, vol. 19, no. 7, pp. 1105–1108, Jul. 2015.
[20] R. G. Gallager, *Information Theory Reliable Communication*. New York, NY, USA: Wiley, 1968.

Aimin Li (Graduate Student Member, IEEE) received the B.E. degree in electronic and information engineering from the Harbin Institute of Technology, Shenzhen, in 2020, where he is currently pursuing the Ph.D. degree with the Department of Electronic Engineering. His research interests include aerospace communications, advanced channel coding techniques, and wireless communications.

Shaohua Wu (Member, IEEE) received the Ph.D. degree in communication engineering from the Harbin Institute of Technology in 2009. From 2009 to 2011, he held a post-doctoral position with the Department of Electronics and Information Engineering, Shenzhen Graduate School, Harbin Institute of Technology, where he has been with since 2012. From 2014 to 2015, he was a Visiting Researcher with BBCR, University of Waterloo, Canada. He is currently a Full Professor with the Harbin Institute of Technology, Shenzhen. He has authored or coauthored more than 100 articles and holds more than 40 Chinese patents. His research interests include wireless image/video transmission, satellite and space communications, advanced channel coding techniques, and B5G wireless transmission technologies.

Jian Jiao (Member, IEEE) received the M.S. and Ph.D. degrees in communication engineering from the Harbin Institute of Technology (HIT), Harbin, China, in 2007 and 2011, respectively. From 2011 to 2015, he was a Post-Doctoral Research Fellow with the Communication Engineering Research Centre, Shenzhen Graduate School, HIT, Shenzhen, China. From 2016 to 2017, he was a China Scholarship Council Visiting Scholar with the School of Electrical and Information Engineering, The University of Sydney, Sydney, Australia. Since 2015, he has been with the School of Electrical and Information Engineering, HIT, where he is currently an Associate Professor. His research interests include error control codes, satellite communications, and massive RA.

Ning Zhang (Senior Member, IEEE) received the B.S. degree from Beijing Jiaotong University, China, in 2007, the M.S. degree from the Beijing University of Posts and Telecommunications in 2010, and the Ph.D. degree from the University of Waterloo, Canada, in 2015. He was a Post-Doctoral Research Fellow with the University of Waterloo and the University of Toronto, Canada, respectively. He is currently an Associate Professor with the University of Windsor, Canada. His research interests include connected vehicles, mobile edge computing, wireless networking, and machine learning. He was a recipient of the Best Paper Award from the IEEE GLOBECOM in 2014, the IEEE WCSP in 2015, the *Journal of Communications and Information Networks* in 2018, the IEEE ICC in 2019, the IEEE Technical Committee on Transmission Access and Optical Systems in 2019, and the IEEE ICCC in 2019. He was the Workshop Chair for MobiEdge'18 (in conjunction with IEEE WiMob 2018), CoopEdge'18 (in conjunction with IEEE EDGE 2018), and 5G&NTN'19 (in conjunction with IEEE EDGE 2019). He serves as an Associate Editor for IEEE INTERNET OF THINGS JOURNAL, IEEE TRANSACTIONS ON COGNITIVE COMMUNICATIONS AND NETWORKING, IEEE ACCESS, and *IET Communications*. He serves as an Area Editor for *Encyclopedia of Wireless Networks* (Springer) and *Cambridge Scholars*. He also serves/served as a Guest Editor for several international journals, such as IEEE WIRELESS COMMUNICATIONS, IEEE TRANSACTIONS ON COGNITIVE COMMUNICATIONS AND NETWORKING, IEEE ACCESS, and *IET Communications*.

Qinyu Zhang (Senior Member, IEEE) received the bachelor's degree in communication engineering from the Harbin Institute of Technology (HIT), Harbin, China, in 1994, and the Ph.D. degree in biomedical and electrical engineering from the University of Tokushima, Tokushima, Japan, in 2003. From 1999 to 2003, he was an Assistant Professor with the University of Tokushima. From 2003 to 2005, he was an Associate Professor with the Shenzhen Graduate School, HIT. He was the Founding Director of the Communication Engineering Research Center, School of Electronic and Information Engineering (EIE). Since 2005, he has been a Full Professor and the Dean of EIE School, HIT. His research interests include aerospace communications and networks, wireless communications and networks, cognitive radios, signal processing, and biomedical engineering. He has been a TPC Member for the Infocom, IEEE ICC, IEEE GLOBECOM, IEEE Wireless Communications and Networking Conference, and other flagship conferences in communications. He was an Associate Chair for Finance of the International Conference on Materials and Manufacturing Technologies 2012. He was the TPC Co-Chair of the IEEE/CIC ICCC 2015. He was the Symposium Co-Chair of the CHINACOM 2011 and the IEEE Vehicular Technology Conference 2016 (Spring). He was the Founding Chair of the IEEE Communications Society Shenzhen Chapter. He is on the Editorial Board of some academic journals, such as *Journal of Communication*, *KSII Transactions on Internet and Information Systems*, and *Science China Information Sciences*.